Computer-aided Decision Support System for Classification of Pigmented Skin Lesions

Qaisar Abbas†

†College of Computer and Information Sciences, Al Imam Mohammad Ibn Saud Islamic University (IMSIU), Riyadh, Saudi Arabia

Summary
Computer-aided decision support systems (CAD-SS) are widely used for providing clinical decision to medical experts. A few CAD-SS systems are developed to diagnosis all categories of pigmented skin lesions (PSLs) using dermoscopy images. These systems are limited to specific categories of PSLs, computationally slow and defined non-effective visual features. In this paper, an improved CAD-SS system is proposed by integrating of effective color and texture features for recognizing of 12 categories of skin lesions. Compared to state-of-the-art systems, the optimal features are extracted from each of PSLs images in a perceptual-oriented color space (CIEL*a*b*). These visual features are then classified by using Learn++ architecture. The CAD-SS system is tested on a total of 360 lesions and achieved an average value of area under the receiver operating curve (AUC) of 0.97. Experimental results indicate that the CAD-SS system yields higher accuracy for recognition of pigmented skin lesions and the CAD-SS system can helpful for less experience dermatologists to take their clinical decisions.

Key words:
Skin Cancer, Computer-aided diagnosis system, Incremental learning, Perceptual color space, Hill-climbing, Color and texture features.

1. Introduction

The recognition of pigmented skin lesions (PSLs) using dermoscopy images [1] has significant improvements during last decades. For early detection of skin cancer, the clinical experts like dermatologists are widely using computer-aided decision support system (CAD-SS) [2] to classify the type of PSLs. In practice, the CAD-SS systems are providing second opinion [3] to less experience dermatologists. To help practitioners, the CAD-SS systems are developed by extraction of visual features to classify melanoma skin lesions. According to review, the CAD-SS systems are extensively studied but they recognized only certain types of pigmented skin [4] lesions. These systems are mainly developed based on extraction of color and texture features [5] and then classified these features using machine learning algorithms. From the last 10 years, the CAD-SS system [6] is also considered as an active and challenging research area in the medical domains.

Manuscript received April 5, 2016
Manuscript revised April 20, 2016

There are 12 main types of pigmented skin lesions when diagnosis through dermoscopy. When the lesion is classified whether it is melanocytic or non-melanocytic lesion then physician must follow to next-level process, the melanocytic lesion as benign, suspect or malignant is characterized as shown in Fig.1. However the automatic extraction of visual features is one of the difficult steps for the development of CAD-SS systems because it may require domain specific knowledge of pattern recognition techniques. Therefore in this paper, extraction and classification of visual features are mainly focused.

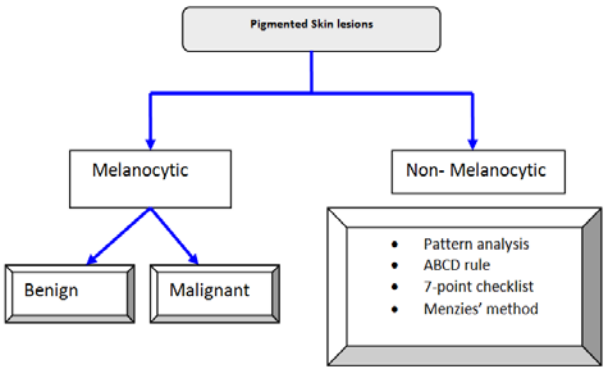

Fig. 1 Algorithm for the differentiation between melanocytic and non-melanocytic lesions

In the past studies, many CAD-SS systems [6-11] were proposed but a few systems were found, which focused on CAD-SS in the domain of dermatology. However, these CAD-SS systems were not developed by using perceptual-oriented or uniform color space but they had utilized non-uniform color space such as RGB, CIELAB or HSV and the color and texture features were not effectively extracted. In the field of dermatology, the extraction of effective texture and color features [12] is a challenging task for querying melanoma versus nevus lesions. In previous researches, a minimum of 168-based features vector is utilized for recognition of melanoma-nevus lesions. In fact, the recognition system is strictly based on direct matching of malignant melanomas or benign lesions without focusing on all types of PSLs. As a result, there is

a dire need to develop an effective and complete CAD-SS system for recognition of all categories of pigmented skin lesions (PSLs).

2. Proposed Architecture

The proposed CAD-SS system is developed based on four major steps such as perceptual-oriented color space transform, extraction of color and texture features; develop a normalized feature vector and finally classification.

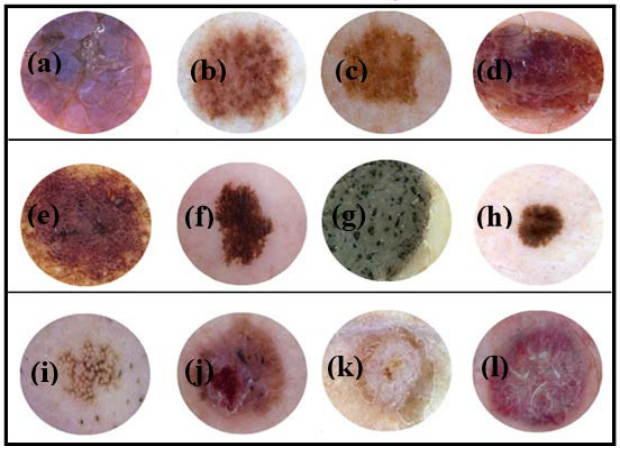

Fig. 2 An example of one ROI image from each dermoscopy image category such as (a) melanoma, (b) atypical nevi, (c) benign nevi, (d) congenital nevi, (e) blue nevi, (f) lentigo, (g) seborrhoeic keratosis (SK), (h) melanocytic nevus, (i) actinic keratosis (AK), (j) basal cell carcinoma (BCC), (k) squamous cell carcinoma (SCC) and (l) markel cell carcinoma (MCC).

In this paper, an affective CAD-SS system is developed based on visual content such as color and texture features extracted in a perceptual-oriented color space for recognition of categories of pigmented skin lesions (PSLs). In this CAD-SS system, the total of 360 PSLs images [13] are utilized in which the melanoma of 30, atypical nevi of 30, benign nevi of 30, congenital nevi of 30, blue nevi of 30, lentigo of 30, seborrhoeic keratosis (SK) of 30, melanocytic nevus of 30, actinic keratosis (AK) of 30, basal cell carcinoma (BCC) of 30, squamous cell carcinoma (SCC) of 30 and markel cell carcinoma (MCC) of 30. From all these images, the extraction of effective 12-color and 6-texture features in total of 18 features are investigated. In this CAD-SS system, the non-uniform RGB image is transformed to perceptual-oriented CIEL*A*B* color space. Afterwards, effective techniques are proposed to extract color and texture features in this CIEL*A*B* color space. After normalizing these features, the CAD-SS system is trying to recognize of a query image by using deep architecture and Learn++ algorithms. The sensitivity, specificity and accuracy statistical metrics are also used for measuring performance of the CAD-SS system on dataset of 360 images.

2.1 Utilization of Dataset

The performance of CAD-SS system for dermoscopy skin lesions is tested on a dataset of 360 dermoscopy images. In this dataset of 360 PSLs, the distribution of each categories are divided into melanomas, atypical nevi, benign nevi, congenital nevi, blue nevi, lentigo, seborrhoeic keratosis, melanocytic nevus, actinic keratosis (AK), basal cell carcinoma (BCC), squamous cell carcinoma (SCC) and markel cell carcinoma (MCC). For these 12 categories of PSLs, each category contains 30 images. These images are mostly selected images as a CD resource from the EDRA Interactive Atlas of Dermoscopy [13], while others are required from different sources. To perform statistical measure, each skin lesion image of varying size is down sampled to (600 × 600) pixels. In JPEG format having 24-bit/pixel, each image is stored to the hard disk in JPEG format. From the center of each image of (600 × 600) pixels, the size of (300 × 300) pixels as region-of-interest (ROI) is automatically selected for performing the process of feature extraction and classification. For example, one PSLs image per category is shown in Fig.2.

2.2 Transforming of Color space

Skin lesions are color images, which are acquired from digital dermoscopy. For characterization of these lesions, color features are played an important role for characterization because color information is of high relevance. Although, the overall appearance of the skin lesion could be erroneously [11] considered the same from patient to patient (brownish lesion and healthy pink skin) the absolute values of these colors differs from person to person. Afterwards, if the method aims to be used in practice, it should not be based on absolute color values but instead it must use relative differences. In this paper, the full color information technique is presented for dermoscopy images. The CAD-SS system is also fully adapted to human perception mainly due to the selection of CIE L*a*b* color space where L* represent the lightness, a* represents the position of the color between red/magenta and green and b* the same respect yellow and blue. Since, this color space was developed to be as related to human perception as possible; it has been shown [14] that some non-uniformity remains in it. To overcome this problem, CIE proposed the use CIE94 [14] and CIEDE2000 [15] color distances instead of the traditional Euclidean one.Despite the fact that CIEDE2000 was developed to further correct CIE L*a*b* remaining non uniformity when compared to CIE94, some authors claim that it is a formula for small color differences [16], [17]

and, that while the CIEDE2000 equation certainly performs better than CIE94 for some data sets, its added complexity is probably not justified form most practical applications [18]. Moreover, Melgosa et al. [19] found that the improvement of CIE94 over Euclidean distance was considerably greater than that of CIEDE2000 over CIE94. These reasons motivated the use of CIE94 in this paper. The mathematical expression of CIE94 is given in Eq. 1.

$$\Delta E_{94}^{*} = \left(\left(\frac{\Delta L^{*2}}{k_L S_L} \right) + \left(\frac{\Delta C_{ab}^{*2}}{k_C S_C} \right) + \left(\frac{\Delta H_{ab}^{*2}}{k_H S_H} \right) \right)^{1/2} \quad (1)$$

Where

$$\Delta H_{ab}^{*2} = 2\sqrt{\Delta C_{ab,r}^{*2} \Delta C_{ab,s}^{*2}} \sin\left(\frac{\Delta h_{ab}}{2} \right) \quad (2) \text{ and}$$

$$h_{ab} = \tan^{-1}\left(\frac{b^*}{a^*} \right), C^* = \left(a^2 + b^2 \right)^{1/2} \quad (3)$$

$$S_L = 1, S_C = 1 + 0.045 C_{ab}^{*}, S_H = 1 + 0.015 C_{ab} \quad (4)$$

$$k_L = k_C = k_H = 1$$

Where, C_{ab} the mean of the reference color chroma C_r and the sample color chroma C_s and L is the corresponding value for lightness. S_L , S_C , and S_H are parametric functions that allow the adaptation of the formula to the experimental data set for whom the equation is derived. K_L , K_C and K_H are weighting factors that are set to one by default that can be changed regarding to viewing conditions. Accordingly, the L*a*b* uniform color space is the color system adopted by the CAD-SS because of its better uniformity and adaptation to human perception.

2.3 Extraction of Color features

After transforming RGB image to CIEL*a*b* perceptual-oriented color space, the color features are extracted. Color features are used in a wide range of image recognition tasks, mainly due to the color of an object or scene and often contained in the image is very relevant.

In addition to this, compared with the other visual features, color characteristics of the image have high importance. In this paper, color coherence, moments and correlation features are derived from each image in CIEL*a*b* perceptual-oriented color space.

Steps	Algorithm 1: Determine color coherency feature
1.	Compare the number of pixels of the current histogram bin with the number of pixels of the neighboring bins.
2.	If the neighboring bins have different numbers of pixels, the algorithm makes an uphill move toward the neighbouring bin with larger number of pixels.
3.	If the immediate neighbouring bins have the same numbers of pixels, the algorithm checks the next neighbouring bins continuing until two neighbouring bins with different numbers of pixels are found. Then, an uphill move is made toward the bin with larger number of pixels.
4.	The uphill climbing is continued (repeat steps 1, 2 and 3) until reaching a bin from where there is no possible uphill movement.
	Conditions: That is the case when the neighboring bins have smaller numbers of pixels than the current bin. Hence, the current bin is identified as a peak (local maximum). Unclimbed bins are selected one by one and steps 1 to 4 are repeated until all non-zero bins of the color histogram are not climbed.
5.	Neighboring pixels that lead to the same peak are grouped together, associating every pixel with one of the identified peaks.
6.	These peaks are saved and serve as the initial cluster centroid positions for the perceptually adapted K-means clustering, whereas the number of clusters is the value of K. The bins of the histogram depend on the parameter specified at the call time of HCA, experimentally fixed here to 6.

2.3.1. Color Coherency Feature

For determining the color coherence presents in lesion, frequency level of six distinct colors (black, red, light brown, dark brown, blue-gray and white) are extracted through Hill climbing algorithm (HCA) [20,21] technique. This technique is utilized and modified in terms of K-means clustering method by using uniform color space CIE L*a*b* with the advanced color difference equation CIE94. To extract color coherency feature, the codebook for K-means algorithm implementation, chosen to minimize the empirical quantization error, can be obtained through an optimization. Due to the nature of the CIE94 color distance formula, a heuristic method based on the direction of the gradient vector has been adopted in the proposed approach. At each image pixel, the gradient vector points in the direction of the largest possible function increase, corresponding its magnitude to the rate of change in that direction. The opposite one corresponds, then, to the direction of the function decrease and therefore it can be used to obtain its local minima. Hence, to find the location of the new codevectors, the algorithm moves from the old centroids in the opposite direction to the gradient. When moving along this direction, the function value will decrease until a local minimum is reached. In that particular moment, if the algorithm keeps moving, the function will increase. This growing in the function's value is an indicator of the approximate location of the new codevector.

As a result of this K-means procedure, every pixel in the image is assigned to one of the color centroids. The value for K is automatically obtained as well as the position of the initial clusters for K-means. To this purpose, HCA

generates the 3D color histogram of the input image in CIE L*a*b* and searches for the peaks on it. The algorithm starts at a non-zero bin of the color histogram and make uphill moves until reaching a peak, which is mentioned above in algorithm 1.
To get colors frequency by using above algorithm, the maximum and minimum segmented regions are used by counting the number of pixels in that area.

2.3.2. Color Moments Feature

The color moments are then extracted using mean and variance of colors in terms of Eigen vectors, which are extracted from each channel of CIEL*a*b* lesions. In fact, the color moments are easiest way to calculate the difference among nevus and malignant lesions. The color moments are calculated using each channel of CIEL*a*b* lesion. Afterwards, two Eigen values (lambda 1, lambda 2) are calculated and selected from these mean and variance color values of each plane of CIEL*a*b* lesion.

2.3.3. Color Correlogram Feature

The color correlation feature is then calculated through color correlogram, which is another way of expressing the image color distribution [22]. This feature is not only depicting pixels representing a color image but also reflects on the spatial correlation between the different colors. Experimental results show that the retrieval efficiency vector color associated with a higher figure than the color histogram and the color moments, particularly consistent query spatial relations image. In practice, this correlogram feature take into account the local color spatial correlation as well as the global distribution of this spatial correlation compared to purely local properties such as pixel position, gradient direction or purely global properties such as color distribution. However in the past studies for CAD-SS systems, there are many developed methods, which are purely based on local properties, which are likely to be sensitive to large appearance changes and other methods are also proposed, which are based on purely global properties is susceptible to false positive matches. In contrast of both local and global properties, the color correlogram is more stable to these changes and prove to be quite effective for content-based image retrieval from a large image database and also for object recognition. In practice, the description of color correlogram feature is defined as a table indexed by color pairs, where the dth entry for every row i and j specifies the column probability of finding a pixel of color at a distance from a pixel of color i in CIEL*a*b* color space image. Therefore, this color correlogram is to calculate color interaction of pixels.

2.4. Extraction of Texture Features

A texture feature is not dependent on visual characteristics or the color image that reflects the luminance homogeneity phenomenon. It is an inherent characteristic of all common patterns, which are available in any type of skin lesions. Therefore, the extraction of texture feature is also an important step for the development of computer-aided diagnosis (CAD) systems. In the past decades, the pattern extraction and recognition steps are performed that have made significant achievements in terms of classification. The texture features are extracted in this paper based on roughness, directionality and linelikeness by Gabor wavelets (GWs) [23]. The GWs are selected for PSLs images because it has been used in many applications for pattern classification.
The L* plane is used from CIEL*a*b* color space image and is represented by GWs technique to extract these features. These three features are utilized, which show very successful results in evaluation of pattern analysis. The detail descriptions of these texture features are explained in the subsequent sections. To extract texture features or patterns from L* lesion, the patterns are defined by both global and local interactions of pixels. The Gabor wavelets (GWs) are utilized in a multi-resolution step with scale and orientation parameter as 6 and 4, respectively to define texture-related features. In Fig.3, examples of Gabor wavelets filter responses are displayed. This figure shows that the GWs are effectively utilized to extract texture features.
In fact these effective features obtained because a spatial domain of GWs (as shown in Fig.4) is generated by specifying the following parameters: scales, orientations and center frequency. If I(x,y) is provided image then discrete Gabor wavelet transform is given by a convolution. Afterwards based on the mean and variance values, two images (μ, λ) are constructed with minimum and maximum intensity variation among them.

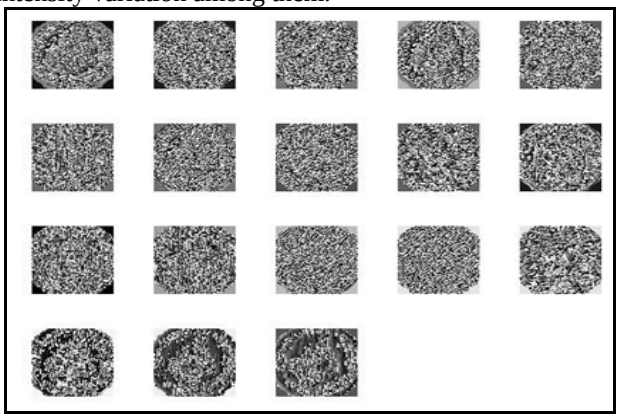

Fig. 3 Example of Gabor wavelets Features that are extracted from different scales.

To calculate the roughness feature, the mean image (μ) is utilized and then take first averages at every point over 8 by 8 neighborhoods pixels. In fact, the roughness has an important characteristics to identify the large texture exists, even where a smaller micro texture exists in a skin lesion. After that, the directionality feature is measured to describe the texture patterns at different orientations. The angle and magnitude are measured using the frequency distribution of oriented local edges against their directional angles. The edge strength and the directional angle are computed using the Sobel edge detector approximating the pixel-wise x- and y-derivatives of the image. Next to extract a measure from this histogram, the sharpness of the peaks are computed from their second moments.

The linelikeness feature is defined as an average coincidence of the edge directions (more precisely, coded directional angles) that co-occurred in the pairs of pixels separated by a distance d along the edge direction in every pixel. The edge strength is expected to be greater than a given threshold eliminating trivial "weak" edges. The coincidence is measured by the cosine of difference between the angles, so that the co-occurrences in the same direction are measured by +1 and those in the perpendicular directions by -1.

Finally, all the features which are extracted from the lesion area are combined into a single feature vector.

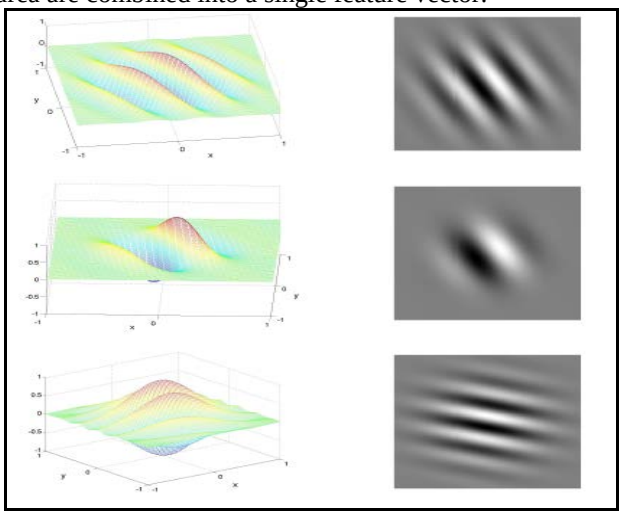

Fig.4 Examples of Gabor filters with different frequencies and orientation in which, first column show 3D plots and second one show the intensity plots of their amplitude along image plane.

2.5. Normalization of Features Vector

These extracted color and texture features are combined into a single features vector (FV) of each image in the dataset and the query image. Afterwards, the normalization step is performed on each features vector to range values between 0 and 1 by dividing the each element to its norm which is the square root of the sum of the square of each element. For each lesion, this normalized feature vector is calculated and stored in a dataset. Furthermore, these feature vectors (FVs) of each lesion are utilized to search and retrieve the most similar records of a query image by using maximum likelihood criteria.

2.6. Classification of visual features

Learn++ [24] multi-class machine learning algorithm is utilized to recognize visual features. The Learn++ classifier is designed based on first creating week classifiers and then combining these classifiers using majority voting technique to take final decision. In practice, Learn++ algorithm has capability to learn new data by modifying the distribution of training dataset in case of availability of new dataset. This intelligent distribution of training dataset makes it different compared to other multi class classifiers. For learning features of CAD-SS system, the incremental learning Learn++ algorithm is effective.

In literature, many ensemble classifiers are utilized. These classifiers were supposed to provide strong classification results based on ensemble of weak classifiers through a procedure called boosting. Using a majority voting technique, these weak classifiers are combined, which are provided better performance compared to other strong classifiers. Moreover, other strong classifiers such as AdaBoost are also suffered overtraining compared to Learn++ algorithm because it is designed to add incremental learning capability to an existing classifier.

After normalization of each features, the features matching step is performed through Learn++ algorithm in this CAD-SS system. This Learn++ algorithm has selected randomly training dataset, weak learners and an integer parameter with value of 12, specifying the number of classifiers to be generated from 360 pigmented skin lesions (PSLs).

In this setup of Learn++ algorithm, neural networks are selected because these are most suitable weak learners, in which layers and/or classification errors are used to control their weakness. In the decision step, top-most n-ranked images are selected by using majority voting, which are matched with the query image. In fact, n-ranked images are selected with highest votes compared to the features of query image. The majority voting mechanism effectively fine-tunes the classification decision from the rough estimates provided by each classifier. For better understanding of Learn++ algorithm, the authors are referred to study this article [24].

3. Experimental Results

The proposed CAD-SS system for pigmented skin lesions (PSLs) is implemented in MATLAB 2015 on Intel(R)

Core (TM) i7-3317 CPU @ 1.7GHz, 1.7GHz, 8 GB RAM and Windows 8, 64-bit operating system. In total, 360 images are contained in the PSLs dataset. All images are down sampled to (600 × 600) pixels and then (300×300) pixels areas from central position are selected and stored in a database before feature extraction step. These 360 PSLs images are contained melanoma of 30, atypical nevi of 30, benign nevi of 30, congenital nevi of 30, blue nevi of 30, lentigo of 30, seborrhoeic keratosis (SK) of 30, melanocytic nevus of 30, actinic keratosis (AK) of 30, basal cell carcinoma (BCC) of 30, squamous cell carcinoma (SCC) of 30 and markel cell carcinoma (MCC) of 30. All 360 image's features are extracted and stored in a file to test the performance of proposed CAD-SS system. The classification decision is performed using Learn++ incremental algorithm. In all PSLs images, the 30% lesions are used to train the Learn++ classifier and 70% are used to test this classifier.

To measures the performances of CAD-SS system, the Sensitivity (SN), Specificity (SP) and area under the curve (AUC) statistical matrices are calculated. The area (AUC) [25] under the receiver operating characteristic analysis is used on the test data set to investigate the sensitivity: SN and specificity: SP. The area under the curve (AUC) is the nearly commonly used index to assess the overall discrimination. The AUC ranges from 0.50 to 1.0 and the greater its value the higher is the accuracy of CAD-SS system. For experimental analysis, the data set is divided into training (30%) and testing (70%). The Table 1 shows the overall average results on all 12 classes of pigmented skin lesions (PSLs) and area under the curve (AUC) is also represented in Fig.3.

Table 1: The average values of Sensitivity (SN), Specificity (SP) and area under the receiver operating curve (AUC) of the CAD-SS system of 360 dermoscopy images

Lesion Type	Sensitivity	Specificity	AUC
1. Melanomas (Ms)	0.97	0.74	0.93
2. Atypical Nevis (ANs)	0.88	0.72	0.90
3. Benign Nevis (BNs)	0.90	0.71	0.88
4. Congenital Nevis (CNs)	0.91	0.72	0.87
5. Blue Nevis (BNs)	0.95	0.69	0.92
6. Lentigo Nevis (LNs)	0.97	0.65	0.95
7. Seborrhoeic keratosis (SK)	0.96	0.64	0.94
8. Melanocytic Nevus (MNs)	0.95	0.61	0.90
9. Actinic keratosis (AK)	0.95	0.60	0.93
10. Basal cell carcinoma (BCC)	0.97	0.68	0.92
11. Squamous cell carcinoma (SCC)	0.97	0.80	0.95
12. Markel cell carcinoma (MCC)	0.9741	0.74	0.96

4. Discussion and Conclusion

The proposed computer-aided decision support system (CAD-SS) is effective for classification of all types of PSLs. The results of the CAD-SS system on this dermoscopy data set containing 360 are shown in Table 1. Table 1 demonstrates that sensitivity: SN, specificity: SP and area under the ROC curve (AUC) analysis are greatly improved by extracting informative visual features. The Fig. 5 has shown the corresponding receiving operating characteristic curve (ROC). Area under the curve (AUC) shows the significant result of this CAD-SS system, which is greater than 0.5. As displayed in Table 1, it can be noticed that in case of Seborrhoeic keratosis (SK), Melanocytic Nevus (MNs), Actinic keratosis (AK), Basal cell carcinoma (BCC), Squamous cell carcinoma (SCC), Markel cell carcinoma (MCC), the best performance have been measured i.e., AUC: 0.95 on average. Furthermore, the average value of AUC i.e, 0.97 in all categories of skin lesions has been improved as compared to state-of-the-art systems. It is because of designing an effective classification solution with optimal color-texture features extraction in a perceptual-uniform color space.

Therefore, this CAD-SS system is giving a valuable and intuitive aid to the clinician in the decision making process. In fact, this system can be useful as a training tool for medical students and inexpert practitioners given its ability to recognize large collections of PSLs images using their visual attributes.

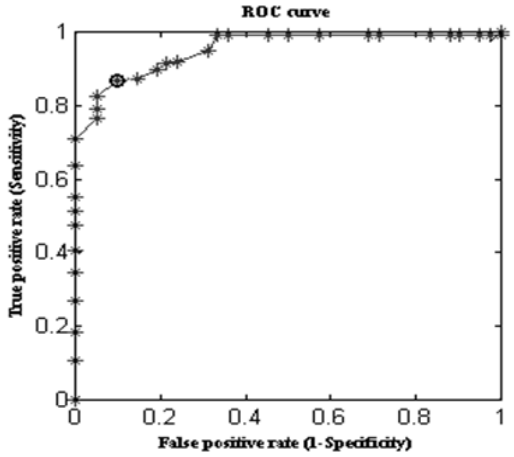

Fig. 5 Area under the receiver operating curve (AUC) for the proposed CAD-SS System.

An improved decision-support system for computer-aided diagnosis (CAD-SS) of pigmented skin lesions (PSLs) images is developed in this paper with greatly enhanced results and that can be used to provide second opinion to less experience dermatologists. In the future work, more color and texture properties will be explored to apply this classification system for both clinical and dermoscopic images.

Acknowledgment

The authors would like to express their cordial thanks to the department of Research and Development (R&D) of IMAM, university for research grant no: 360905.

References

[1]. A. Masood and A. Ali Al-Jumaily, "Computer Aided Diagnostic Support System for Skin Cancer: A Review of Techniques and Algorithms," International Journal of Biomedical Imaging, vol. 2013, pp. 1–22, 2013.

[2]. D. Ruiz, V. Berenguer, A. Soriano, B. Sánchez, "A decision support system for the diagnosis of melanoma: A comparative approach," Expert Systems with Applications, vol. 38, pp.15217–15223, 2011.

[3]. S. Dreiseit, M.Binder, "Do physicians value decision support? A look at the effect of decision support systems on physician opinion," Artificial Intelligence in Medicine, vol. 33, pp. 25–30, 2005.

[4]. L. K. Ferris, J.A. Harkes, B. Gilbert, D.G. Winger, K. Golubets, O. Akilov, M. Satyanarayanan, "Computer-aided classification of melanocytic lesions using dermoscopic images," Journal of the American Academy of Dermatology, vol. 73, pp. 769–776, 2015.

[5]. W.V. Stoecker, M. Wronkiewiecz, R. Chowdhury, R.J. Stanleyb, J. Xu, A. Bangert, B. Shrestha et al., "Detection of granularity in dermoscopy images of malignant melanoma using color and texture features," Computerized Medical Imaging and Graphics, vol. 35, pp. 144–147, 2011.

[6]. N.K. Mishra, M.E. Celebi, "An overview of melanoma detection in dermoscopy images using image processing and machine learning," Computer Vision and Pattern Recognition, 2016.

[7]. J. Premaladh, K. S. Ravichandran, "Novel approaches for diagnosing melanoma skin lesions through supervised and deep learning algorithms," Systems-Level Quality Improvement," Journal of Medical Systems, 2016.

[8]. M. Filho, Z. Ma, J. Manuel, R. S. Tavares, "A Review of the Quantification and Classification of Pigmented Skin Lesions: From Dedicated to Hand-Held Devices," Mobile Systems, Journal of Medical Systems, vol. 39:177, 2015.

[9]. M. Tarjoman, E. Fatemizadeh, K. Badie, "An implementation of a CBIR system based on SVM learning scheme," J Med Eng Technol, vol. 37, pp. 43–47, 2013.

[10]. K. Bunte, M. Biehl, M.F. Jonkman, N. Petkov, "Learning effective color features for content based image retrieval in dermatology," Pattern Recognition, 44, pp.1892–1902, 2011.

[11]. Q. Abbas, M.E. Celebi, C. Serrano, I. Garcia, G. Ma, "Pattern classification of dermoscopy images: A perceptually uniform model," Pattern Recognition, vol. 46, pp. 86–97, 2013.

[12]. C. Serrano, B. Acha B, "Pattern analysis of dermoscopic images based on markov random fields," Pattern Recognition, vol. 42, pp.1052–1057, 2009.

[13]. G. Argenziano, H.P. Soyer, V. De Giorgi, D. Piccolo, P. Carli, M. Delfino et al, "Interactive atlas of dermoscopy CD. Milan: EDRA Medical Publishing and New Media," 2000.

[14]. R. McDonald and K. J. Smith, "CIE94 - A new colour-difference formula," J. Soc. Dyers Col., vol. 111, pp.376–379, 1995.

[15]. M. R. Luo, G. Cui, B. Rigg, "The development of the CIE 2000 colour-difference formula: CIEDE2000," Color Research & Application, vol. 26, pp.340–350, 2001.

[16]. G. Sharma, W. Wu and E. N. Dalal, "The CIEDE2000 color-difference formula: Implementation notes, supplementary test data, and mathematical observations," Color Res. Appl., vol. 30, pp.21–30, 2005.

[17]. J. Schanda, "International commission on illumination. Colorimetry: understanding the CIE system," John Wiley Sons, New Jersey, 2007.

[18]. M. D. Fairchild, "Color Appearance Models," Wiley-IS&T, 82, 2005.

[19]. M. Melgosa, R. Huertas and R. S. Berns, "Relative significance of the terms in the CIEDE2000 and CIE94 color difference formulas," J. Opt. Soc. Am. A-Opt.Image Sci. Vis., vol. 21, pp.2269–2275, 2004.

[20]. T. Ohashi, Z. Aghbari, A. Makinouchi, "Hill-climbing algorithm for efficient color based image segmentation," IASTED International Conference on Signal Processing, Pattern Recognition, and Applications," 2003.

[21]. Z. A. Aghbari, R. Al-Haj, "Hill-manipulation: an effective algorithm for color image segmentation," Image Vis Comput, vol. 24, pp.894–903, 2006.

[22]. J. Amores, N. Sebe, P. Radeva, "Context based object-class recognition and retrieval by generalized correlograms," IEEE Transactions on Pattern Analysis and Machine Intelligence, vol. 29, pp. 1818–1833, 2007.

[23]. F. Riaz, A. Hassan, S. Rehman and U. Qamar, "Texture classification using rotation- and scale-invariant gabor texture features," IEEE Signal Processing Letters, vol. 20, pp. 607–610, 2013.

[24]. R. Polikar, L. Udpa, S.S. Udpa, V. Honavar, "Learn++: an incremental learning algorithm for supervised neural networks," IEEE Trans Syst Man Cybern C., vol. 31, pp.497–508, 2001.

[25]. A. P. Bradley, "The use of the area under the ROC curve in the evaluation of machine learning algorithms," Pattern Recognition, vol. 30, pp.1145–1159, 1997.

Qaisar Abbas received his BSc and MSc degrees in Computer Science from Bahauddin Zakariya University(BZU), Pakistan in 2001, 2005; respectively. He then became the Lecturer and Software developer in the same department. He has completed PhD in the school of Computer Science and Technology at the Huazhong University of Science and Technology (HUST), Wuhan China. He is now working as an assistant professor in College of Computer and Information Sciences, Al Imam Mohammad Ibn Saud Islamic University (IMSIU), Riyadh, Saudi Arabia. His research interests include: image processing, medical image analysis, Genetic programming and pattern classification.